ARL-TR-9529 • Sep 2022

DEVCOM ARMY RESEARCH LABORATORY

Range Estimation of an Ultraviolet Communication Source using a Mobile Sensor

by Terrence J Moore, Fikadu T Dagefu, Hakan Arslan, Michael J Weisman, and Robert J Drost

NOTICES

Disclaimers

The findings in this report are not to be construed as an official Department of the Army position unless so designated by other authorized documents.

Citation of manufacturer's or trade names does not constitute an official endorsement or approval of the use thereof.

Destroy this report when it is no longer needed. Do not return it to the originator.

ARL-TR-9529 ● SEP 2022

Range Estimation of an Ultraviolet Communication Source using a Mobile Sensor

by Terrence J Moore, Fikadu T Dagefu, Michael J Weisman, and Robert J Drost
Army Research Directorate, DEVCOM Army Research Laboratory

Hakan Arslan
Oak Ridge Associated Universities (ORAU)

REPORT DOCUMENTATION PAGE

Form Approved
OMB No. 0704-0188

1. REPORT DATE *(DD-MM-YYYY)*	2. REPORT TYPE	3. DATES COVERED (From - To)
September 2022	Technical Report	March 2021-September 2021

4. TITLE AND SUBTITLE
Range Estimation of an Ultraviolet Communication Source using a Mobile Sensor

5a. CONTRACT NUMBER

5b. GRANT NUMBER

5c. PROGRAM ELEMENT NUMBER

6. AUTHOR(S)
Terrence J Moore, Fikadu T Dagefu, Hakan Arslan, Michael J Weisman, and Robert J Drost

5d. PROJECT NUMBER
AH80

5e. TASK NUMBER

5f. WORK UNIT NUMBER

7. PERFORMING ORGANIZATION NAME(S) AND ADDRESS(ES)
DEVCOM Army Research Laboratory
ATTN: FCDD-RLC-NT
Adelphi, MD 20783

8. PERFORMING ORGANIZATION REPORT NUMBER
ARL-TR-9529

9. SPONSORING/MONITORING AGENCY NAME(S) AND ADDRESS(ES)

10. SPONSOR/MONITOR'S ACRONYM(S)

11. SPONSOR/MONITOR'S REPORT NUMBER(S)

12. DISTRIBUTION/AVAILABILITY STATEMENT
Approved for public release; distribution is unlimited.

13. SUPPLEMENTARY NOTES
primary author's email: <terrence.j.moore.civ@army.mil>.

14. ABSTRACT
Ultraviolet (UV) communications has been proposed as a promising modality for short-range military communications, as it is often presumed to have low-probability-of-detection characteristics, has desirable non-line-of-sight properties, and resides within an underutilized frequency band. Recent research efforts have sought to formalize the first presumption of the detection of UV communications. This effort seeks to begin the study of the localization of UV communication sources after they are detected. We focus here exclusively on the range-estimation problem. Using a phenomenon relating UV received power and range over short-to-medium distances ($\ll 1\,\mathrm{km}$), we develop a simple range estimator using the received signal strength. We also theoretically study the performance of the estimator using the Cramér-Rao bound, via simulations, and using previously collected data.

15. SUBJECT TERMS
localization, range estimation, ultraviolet communications, Cramér-Rao bound, root mean-square error

16. SECURITY CLASSIFICATION OF:			17. LIMITATION OF ABSTRACT	18. NUMBER OF PAGES	19a. NAME OF RESPONSIBLE PERSON
a. REPORT	b. ABSTRACT	c. THIS PAGE			Terrence J Moore
Unclassified	Unclassified	Unclassified	UU	19	19b. TELEPHONE NUMBER (Include area code) 240-247-7438

Contents

List of Figures

1. Introduction

Passive source localization is an often studied research problem in radio, optical, and acoustic sensor networks. A common approach[1–3] is indirect estimation based on direct measurements, such as received signal strength (RSS), direction of arrival, time of arrival, time difference of arrival, and frequency difference of arrival. For example, RSS measurements can be converted to estimates of the range from a target source to individual sensors (or groups of sensors) that can be collectively used for localization.

Ultraviolet (UV) communications (over optical wavelengths of, say, 200–$300\,\mathrm{nm}$) and networking has received increasing interest as it offers a robust short-range non-line-of-sight (NLOS) alternative communication modality when radio frequency is unavailable. Unfortunately, despite decades of research, the literature is still lacking with respect to some basic signal processing tasks of signals at the UV wavelengths, such as source localization. To the best of our knowledge, currently only one approach for locating a UV-emitting source has been published. In particular, Zhao et al.[4] estimate the range between unmanned aerial vehicles using a Lambert W function (or omega function) to solve for the range in a reformulation of the usual expression determining the received UV link communication power. This approach can work for line-of-sight (LOS) and NLOS cases, but requires knowledge of various other parameters, including the transmitted and received power, the atmospheric scattering and absorption coefficients, and the geometry of the link in the NLOS case (i.e., the inclination and azimuth angles, as well as the transmitter beamwidth and receiver field of view). Hence, there is an assumption of cooperation between the source and sensor.

We present a simple scheme to estimate the range to a stationary UV source from a single mobile sensor (or UV detector) without such cooperation. Various UV experiments have demonstrated an approximate relationship between the received photon count λ and the range (or distance) r between the UV transmission source and the sensor or receiver.[5–8] An example measurement of this phenomenon is shown in Fig. 1 for the NLOS case. (Details of this example, originally described in the work of Arslan et al.,[9] are discussed in Section 5.) If the system geometry is preserved and only the distances are proportionally increased or decreased, then over a short

range there exists the following approximate relationship:

$$\lambda \propto r^{-\alpha}, \tag{1}$$

where the exponent is $\alpha = 1$ in the single-scattering NLOS case and $\alpha = 2$ in the LOS case for $r \ll 1\,\mathrm{km}$.[10] We use this observation to estimate the range to the UV source by sampling the mean photon count (or received power) at different positions. We also present a performance bound and study the performance via simulations.

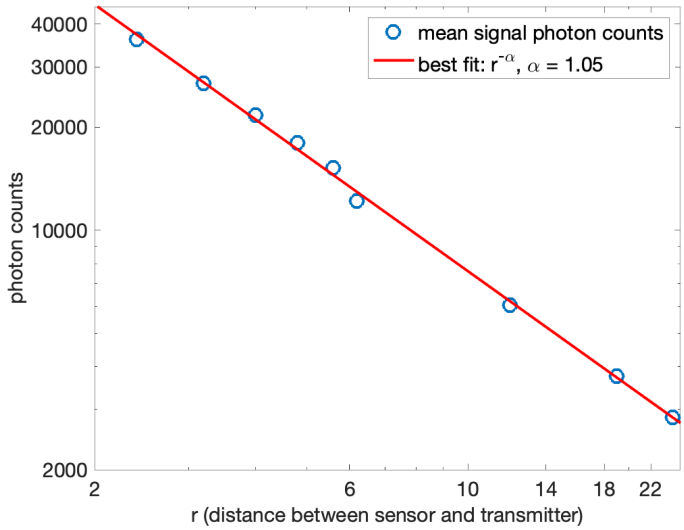

Fig. 1 Mean received photon count versus range for a NLOS scenario presented in the work of Arslan et al.[9] and described in Section 5

2. UV Link Model

In this section, we provide a brief description of the UV link geometry and model. We shall limit the presentation in this work to the short-to-medium range ($r \ll 1\,\mathrm{km}$), single-scattering scenario where the exponent in Eq. 1 is $\alpha = 1$, but the presentation can be easily modified to include the LOS and potentially the multiscattering NLOS cases. In this single scattering case, the assumption is that the receiver only (or mostly) receives photons from the transmitter that have been scattered only once by atmospheric particles. More details of this and the other scenarios are presented elsewhere.[9]

Figure 2 depicts the typical UV link geometry of a transmitter (Tx) and receiver (Rx) separated by a distance r. The figure shows several relevant parameters, including the azimuth and inclination angles of the transmitter $(\phi_{\mathrm{T}}, \theta_{\mathrm{T}})$ and the receiver $(\phi_{\mathrm{R}}, \theta_{\mathrm{R}})$, the Tx beamwidth β_{T}, the Rx field of view β_{R}, and, of course, the range r.

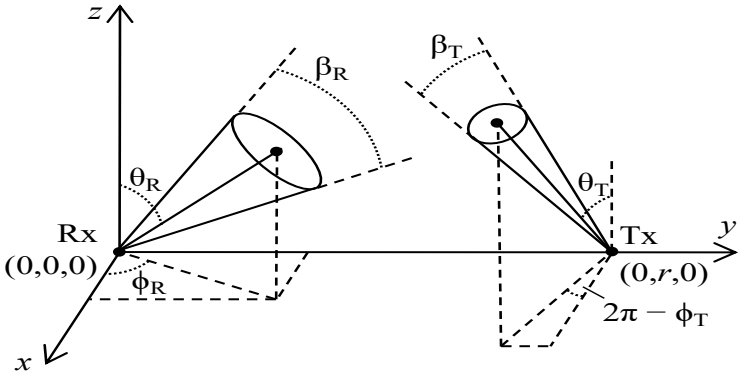

Fig. 2 UV link geometry shown in the work of Drost et al.[11]

The received signal power depends on these parameters in the geometry, as well as system and environment (or channel) parameters. System parameters include the transmitted power P_{T}, the quantum efficiency of the photon multiplier tube (PMT) detector at the receiver, the filter efficiency of the receiver, and the receiver aperture area A_{R}. Environment parameters include the atmospheric scattering coefficient K_{s} and the atmospheric extinction parameter K_{e}. These parameters determine the power received at the sensor.

For simplicity, as considered in the work of Zhao et al.,[4] we consider the configuration in Fig. 2 under the assumption of azimuthal alignment between the Tx and Rx, i.e., $\phi_{\mathrm{T}}, \phi_{\mathrm{R}} \in \{\pm\frac{\pi}{2}\}$. Under this condition, a close approximation for the received optical power P_{R} was derived in the work of Xu[10] and is given by

$$P_{\mathrm{R}} = \frac{P_{\mathrm{T}} A_{\mathrm{R}} K_{\mathrm{s}} \beta_{\mathrm{R}} \beta_{\mathrm{T}}^2 \sin(\theta_{\mathrm{T}} + \theta_{\mathrm{R}})}{32\pi^3 r \sin\theta_{\mathrm{T}} (1 - \cos\frac{\beta_{\mathrm{T}}}{2})} e^{-\frac{K_{\mathrm{e}} r (\sin\theta_{\mathrm{T}} + \sin\theta_{\mathrm{R}})}{\sin(\theta_{\mathrm{T}} + \theta_{\mathrm{R}})}}. \tag{2}$$

This received power can be converted into the mean number of photons received over a specified time period by the sensor. The number of photons received over a given time interval can be modeled as a Poisson distribution. In addition to the shot noise, there also exists additive environment noise due to external sources, such as out-of-band solar noise depending on the filter efficiency. This noise is also modeled

as a Poisson distribution.

To estimate the range from the received power from the simple expression in Eq. 2 requires significant cooperation from the source. Without the knowledge of the parameters gained from this cooperation, the sensor (Rx node) is unaware of any system parameters and is limited to the collection of readings at different positions. This is similar to RSS-based approaches, where the sensor will only be able to measure the received power (equivalently the number of photons collected) and the relative distances in the positions where measurements were collected. The sensor can then estimate the range utilizing the phenomenon, mentioned in Section 1, relating the received number of photons to the range. Details of this proposed method are presented in the following section.

3. Estimation of the Range

To estimate the range, we use the observation that, for the single-scatter NLOS UV link, the mean signal photon count is inversely proportional to the distance between the transmitter and receiver. Under the assumption that the geometry is preserved (i.e., only the range is changed along the y-axis dimension of Fig. 2), when the sensor takes measurements at different ranges as in Fig. 3, the inverse proportion in Eq. 1 with $\alpha = 1$ implies that

$$\lambda_0 r_0 = \lambda_1 r_1, \tag{3}$$

where λ_0 is the true mean photon count at initial range r_0 and λ_1 is the true mean photon count at current range r_1. The displacement between the two measurement positions is given by $\Delta = r_1 - r_0 > 0$ and is known to the sensor. Substituting $r_1 - \Delta$ for r_0 and replacing the true photon count means λ_0 and λ_1 with sample means $\overline{\lambda}_0$ and $\overline{\lambda}_1$ from measurements into Eq. 3 provides an estimate for the range r_1:

$$\overline{\lambda}_0(r_1 - \Delta) = \overline{\lambda}_1 r_1 \implies \widehat{r}_1 = \frac{\Delta\overline{\lambda}_0}{\overline{\lambda}_0 - \overline{\lambda}_1}. \tag{4}$$

However, the sensor actually measures samples of the Poisson means $\lambda_0 + \mu$ and $\lambda_1 + \mu$ due to ambient noise in the atmosphere. The sensor needs to also estimate the mean ambient noise parameter μ. This modifies the formula in Eq. 4 to

$$\widehat{r}_1 = \frac{\Delta(\overline{\nu}_0 - \overline{\mu})}{\overline{\nu}_0 - \overline{\nu}_1}, \tag{5}$$

where $\overline{\mu}$ is the sample mean of the ambient noise parameter μ and $\overline{\nu}_i$ is the sample mean of the signal plus noise parameter $\nu_i = \lambda_i + \mu$ for $i = 0, 1$. Note, the estimate $\widehat{r}_0$ is obtained by replacing $\overline{\nu}_0$ with $\overline{\nu}_1$ in the numerator of the RHS of Eq. 5.

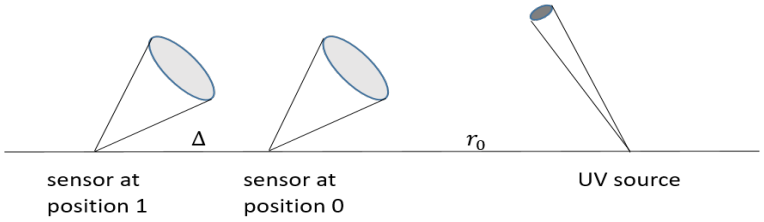

Fig. 3 The sensor takes UV measurements at two different positions at unknown ranges r_0 and $r_1 = r_0 + \Delta$, where the displacement Δ is known

4. Cramér-Rao Bound

In the scenario considered in this work, where the sensor is unaware of any of the system parameters, range estimation performance is determined by the ability to estimate the Poisson parameter determining the received number of photons at each position, as well as the Poisson parameter associated with the ambient noise. It is well known that the sample mean of the measurements of a Poisson random variable is a minimum variance unbiased estimator.* Hence, the sample mean is efficient with variance equal to the Cramér-Rao bound (CRB), which for n samples from a Poisson distribution with parameter λ is given by λ/n.

Under the model assumptions for the zero-azimuth case, the range parameter r_1 can be expressed as a function of the Poisson parameters λ_0, λ_1, and μ in the estimator in Eq. 5. The performance of the estimate $\widehat{r}_1$ can then be found from a transformation of parameters on the CRB[12–14] by taking the gradient of $r_1(\lambda_0, \lambda_1, \mu)$ in Eq. 5 with respect to the parameters. This CRB of the estimate is given by $\partial r_1/\partial \boldsymbol{\theta}^T \cdot \boldsymbol{I}^{-1}(\boldsymbol{\theta}) \cdot \partial r_1/\partial \boldsymbol{\theta}$, where $\boldsymbol{\theta} = [\lambda_0, \lambda_1, \mu]^T$ and the Fisher information $\boldsymbol{I}(\boldsymbol{\theta})$ is diagonal with entries n/λ_0, n/λ_1, and m/μ. When the sensor takes n samples at each position to estimate the Poisson parameters $\nu_0 = \lambda_0 + \mu$ and $\nu_1 = \lambda_1 + \mu$ and m samples to estimate the ambient noise Poisson parameter μ, then the lower bound on mean-square error performance, as determined by the CRB, is given by

$$\mathrm{CRB}(r_1) = \frac{\Delta^2 \lambda_0 \lambda_1 (\lambda_0 + \lambda_1)}{n(\lambda_0 - \lambda_1)^4} + \frac{\Delta^2 (\lambda_0^2 + \lambda_1^2)\mu}{n(\lambda_0 - \lambda_1)^4} + \frac{\Delta^2 \mu}{m(\lambda_0 - \lambda_1)^2}, \tag{6}$$

*This is a consequence of the sum of observations of a Poisson random variable being a complete and sufficient statistic and the Lehmann-Scheffé theorem.[12]

where the first term on the RHS is the bound for the noiseless case (when $\mu = 0$), the second term accounts for the existence of the ambient noise, and the final term is the error due to estimating the ambient noise (as $m \to \infty$ then $\hat{\mu} \to \mu$ and the last term of Eq. 6 vanishes, but the second term remains). Note, even though the estimates of the Poisson means ν_0, ν_1, and μ are minimum variance unbiased estimators, the estimate $\widehat{r}_1$ in Eq. 5 is not guaranteed to be the same. Note, the CRB for r_0 is identical to that for r_1, which means it is greater relative to the distance since $r_0 < r_1$.

5. Results

To test the performance of the estimator, we simulate observed photon counts received by the sensor. We assume the source transmit power is $P_{\mathrm{T}} = 14\,\mathrm{mW}$ with a wavelength of $\ell = 265\,\mathrm{nm}$. At this wavelength, the number of photons transmitted per second is given by $P_{\mathrm{T}}/(hc/\ell)$, where h is Planck's constant and c is the speed of light. For a given configuration of the UV link model in Fig. 2, we utilize the Monte Carlo method described in the work of Drost et al.[11] to calculate the channel gain Γ. Here, we make the following system assumptions: the absorption coefficient is $k_{\mathrm{a}} = 2.8275 \times 10^{-4}\,\mathrm{m}^{-1}$; the Rayleigh scattering coefficient is $k_{\mathrm{r}} = 2.4702 \times 10^{-4}\,\mathrm{m}^{-1}$; the Mie scattering coefficient is $k_{\mathrm{m}} = 1.8275 \times 10^{-4}\,\mathrm{m}^{-1}$; the model parameters in the generalized Rayleigh phase function and the generalized Henyey-Greenstein phase function modeling the Rayleigh and Mie scattering are $\gamma = 0.017$, $f = 0.5$, and $g = 0.72$; the transmitter beamwidth is 21°; and the detector has a field of view of 38.875°, a circular aperture of radius $1\,\mathrm{cm}^2$, and receiver efficiency $\eta = 0.125$[2]. The model also requires the range between the transmitter and receiver, as well as their respective inclination and azimuth angles. For the scenario considered here, we set the transmitter inclination to be 0° (pointing straight up) and the sensor receiver inclination and azimuth angles to be, respectively, 60° and 90° (pointed toward the transmitter). Given the system parameters, the mean number of photons received at the sensor is calculated to be

$$\lambda = (\#\text{ of photons transmitted}) \times \Gamma \times \eta. \tag{7}$$

Observations of photon counts at the sensor are then generated from a Poisson random variable using the above calculated mean. In addition to the shot noise from the signal, we generate a Poisson random variable with mean $\mu = 100$ that models

the background noise in the atmosphere, and we assume this is estimated with the same number of samples as the signal plus noise estimates, that is, $m = n$. The results are averaged over 100 simulation runs.

Figure 4 presents the performance of the estimator, in terms of the root mean squared error (RMSE) and the root CRB (or square-root of the CRB), at different ranges when the displacement between the two measurements is $\Delta = 5\,\mathrm{m}$. The performance degrades as expected when the range r increases with Δ fixed; this degradation is approximately exponential with range. As the number of samples n doubles, the root CRB scales by $1/\sqrt{2}$, as seen from Eq. 6. However, the estimator performance does not improve at the same rate, and we observe that the efficiency (in this case, the ratio of the CRB to the mean squared error) also degrades as n increases. The results in Fig. 4 demonstrate the difficulty of the problem when compared with the cooperative approach presented in the work of Zhao et al.[4] The ranging error experienced in the uncooperative approach here is 5 to 10 times worse than the results from the cooperative scenario (see Fig. 7 in the work of Zhao et al.[4]). However, in that scenario, everything is known, including the transmitter characteristics, the corresponding angles of the geometry, and the environmental conditions, whereas in the scenario considered here, none of this information is assumed or given.

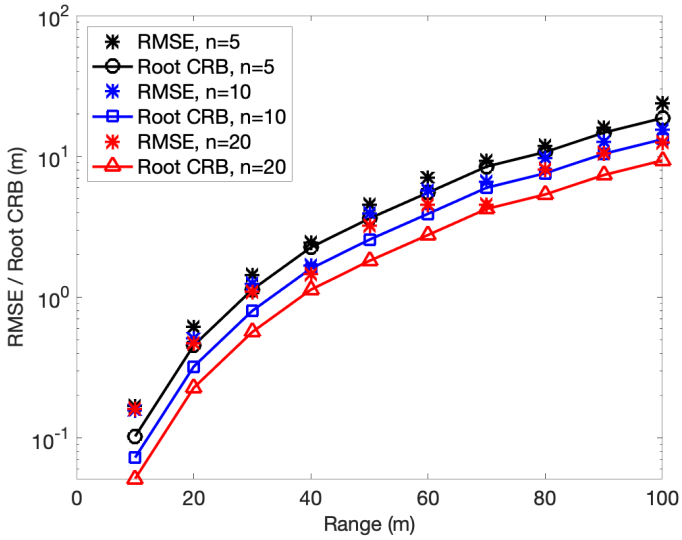

Fig. 4 The RMSE and CRB of the estimate vs. range r_0 with fixed displacement $\Delta = 5\,\mathrm{m}$ between measurements and varying number of samples n

Figure 5 presents the performance of the estimator at different displacements between the two measurements Δ for different ranges r_0; the number of samples is fixed at $n = 10$. The results are as expected: as Δ increases, both the root CRB and RMSE decrease. Note from the CRB in Eq. 6 that while increasing Δ increases the bound, it also results in a greater difference between the photon counts in the denominator. From Eq. 3, we can approximate that this photon count difference scales with Δ as $\lambda_0 \Delta / r_1$. This is ultimately why the RMSE and root CRB decrease as Δ increases. We also note the performance expectation, again based on observations characterized in Eq. 1 and Eq. 3, that as the range halves, the photon count measurements should approximately double, and this behavior is indeed observed in the figure.

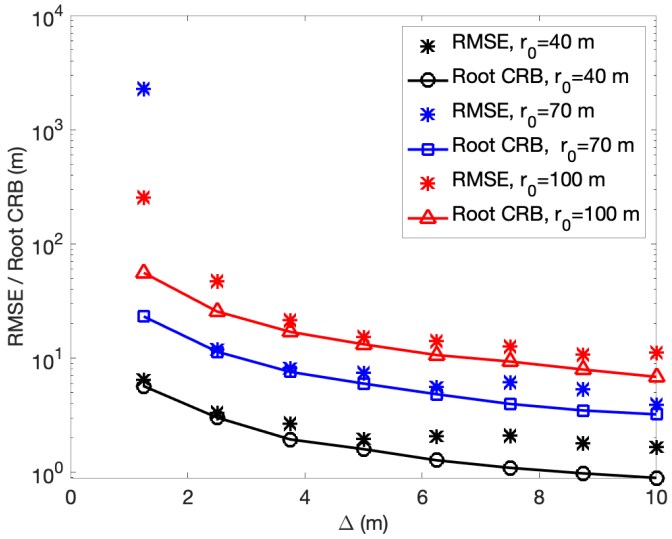

Fig. 5 The RMSE and CRB of the estimate vs. the displacement Δ at varying ranges r_0 and fixed number of samples n

In addition to the simulation results described, we evaluate the estimate on the data collected in the work of Arslan et al.[9] and used to generate Fig. 1. In this experiment, the receiver inclination angle was set to 10° with azimuth angle 90° (toward the transmitter) and the transmitter inclination angle was set to 10° with azimuth angle -90° (toward the receiver). The range positions selected from this experiment are $2.4, 3.2, 4.0, 4.8, 5.6, 6.2, 12.0, 19.0,$ and $24.2\,\mathrm{m}$ separating the transmitter and receiver. At each position, measurements were taken of both the UV source signal and the background noise, that is, ν_i and μ. These measurements were split into group sets to generate runs for the experiment with samples for signal plus noise and

for the noise at each position. The RMSE results are presented in Fig. 6 for $n = 5$ and $n = 10$. In some instances, the noise photon count was excessive, exceeding the mean count attributed to the signal, which is particularly evident in the samples taken at 5.6 and $6.2\,\mathrm{m}$. There is slight improvement when the number of samples increases. The estimated root CRB uses the mean of the entire sample at each position as the "true" value of the parameter, which is unknown. These estimated root CRB values generally track the behavior of the estimator.

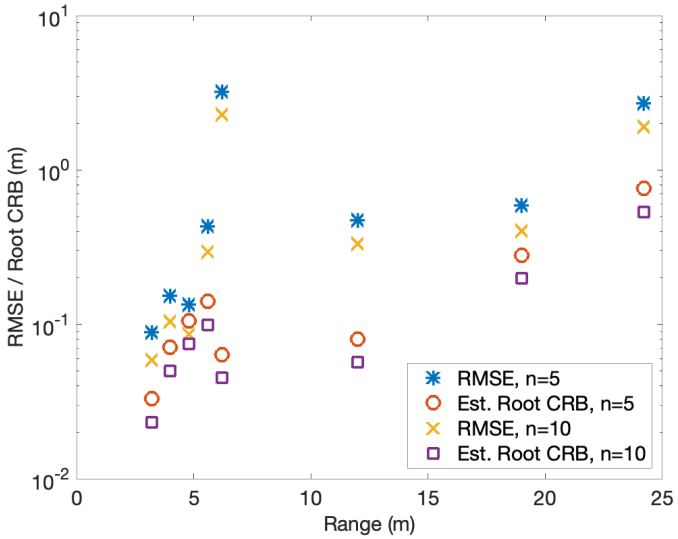

Fig. 6 The RMSE and estimated CRB from data collected in the work of Arslan et al.[9] demonstrating the power-law phenomena observed in Fig. 1

6. Conclusion

With the increasing interest in utilizing the UV spectrum for military communications, there is a need to develop and improve approaches for detection, localization, identification, and so on, of unknown UV communication source targets. The work presented here can be applied to, for example, the case of an autonomous sensor vehicle that discovers a target and seeks to locate the source by first obtaining range estimates. The performance of the straightforward approach considered here degrades significantly as the range increases (e.g., see Fig. 4) but is enhanced with increasing displacement between measurement positions (e.g., see Fig. 5). An improved range estimate can also be obtained by using more samples to improve the photon count estimate. However, if the UV source communication time is brief, then more samples or more time to move the sensor may not be feasible. Future

work includes investigating the use of two (or more) well-spaced and fixed sensors to characterize the associated benefit, as well as examining the localization-from-range multistep estimation problem in this UV source target context. Another avenue of investigation is the adaptation of one of the myriad multipath approaches to localization in NLOS environments.

7. References

1. Porat B, Nehorai A. Localizing vapor-emitting sources by moving sensors. IEEE Transactions on Signal Processing. 1996;44(4):1018–1021.

2. Stoica P, Li J. Lecture notes-source localization from range-difference measurements. IEEE Signal Processing Magazine. 2006;23(6):63–66.

3. Hioka Y, Kishida M. Direction of arrival estimation of harmonic signal using single moving sensor. In: 2014 IEEE 8th Sensor Array and Multichannel Signal Processing Workshop (SAM); 2014 Jun 22-25; A Coruña, Spain. IEEE; 2014. p. 1–4.

4. Zhao T, Yu X, Liu P, Liu L. Ultraviolet anti-collision and localization algorithm in UAV formation network. Optik. 2019;192:162919.

5. Siegel AM, Shaw GA, Model J. Short-range communication with ultraviolet LEDs. In: Ferguson IT, Narendran N, DenBaars SP, Carrano JC, editors. Fourth International Conference on Solid State Lighting; Vol. 5530; 2004 Oct 20; Denver, CO. SPIE; 2004. p. 182–193.

6. Shaw GA, Siegel AM, Model J, Greisokh D. Recent progress in short-range ultraviolet communication. In: Carapezza EM, editor. Unattended Ground Sensor Technologies and Applications VII; Vol. 5796; 2005 Mar 28-Apr 1; Orlando, FL. SPIE; 2005. p. 214–225.

7. Chen G, Xu Z, Ding H, Sadler BM. Path loss modeling and performance trade-off study for short-range non-line-of-sight ultraviolet communications. Optics Express. 2009;17(5):3929–3940.

8. He Q, Xu Z, Sadler BM. Performance of short-range non-line-of-sight LED-based ultraviolet communication receivers. Optics Express. 2010;18(12):12226–12238.

9. Arslan CH, Dagefu FT, Weisman MJ, Drost RJ. Channel model validation for and extensions of an ultraviolet networking optimization framework. In: 2019 IEEE 90th Vehicular Technology Conference (VTC2019-Fall); 2019 Sep 22-25; Honolulu, HI. IEEE; 2019. p. 1–7.

10. Xu Z. Approximate performance analysis of wireless ultraviolet links. In: 2007 IEEE International Conference on Acoustics, Speech and Signal Processing-ICASSP'07; Vol. 3; 2007 Apr 15-20; Honolulu, HI. IEEE; 2007. p. III–577–III–580.

11. Drost RJ, Moore TJ, Sadler BM. UV communications channel modeling incorporating multiple scattering interactions. Journal of the Optical Society of America A. 2011;28(4):686–695.

12. Shao J. Mathematical statistics. Springer; 2003.

13. Moore Jr TJ. A theory of Cramér-Rao bounds for constrained parametric models. University of Maryland, College Park; 2010.

14. Kay SM. Fundamentals of statistical signal processing. Prentice Hall PTR; 1993.

1 (PDF)	DEFENSE TECHNICAL INFORMATION CTR DTIC OCA
1 (PDF)	DEVCOM ARL FCDD RLD DCI TECH LIB
1 (PDF)	ORAU H ARSLAN
4 (PDF)	DEVCOM ARL FCDD RLC NT T J MOORE F T DAGEFU M J WEISMAN R J DROST